Adsorptive Denitrogenation of Light Gas Oil by Silica-Zirconia Cogel

Youn-Sang Bae, Min-Bae Kim, Hyun-Jung Lee, and Chang-Ha Lee
Department of Chemical Engineering, Yonsei University, 134 Shinchon-dong, Seodaemun-gu, Seoul, 120–749, Korea

Jae Wook Ryu
SK Corporation, 140–1 Wonchon-dong, Yusung-gu, Taejon, 305–712, Korea

DOI 10.1002/aic.10642
Published online September 15, 2005 in Wiley InterScience (www.interscience.wiley.com).

The characteristics of adsorption and desorption of nitrogen-containing compounds (NCCs) on the Si-Zr cogel were studied with regard to denitrogenation of light gas oil (LGO) through batch and dynamic experiments. The Si-Zr cogel adsorbent showed a high selectivity of NCCs due to the role of the zirconia on the cogel, regardless of the amount and types of sulfur-containing compounds (SCCs) in the LGO. When the temperature increased from 283 to 323 K, the adsorbed amount of NCCs increased and the time taken to reach the adsorption equilibrium grew shorter. On the other hand, the adsorbent regeneration by the solvent grew worse at higher temperatures when the desorption temperature was applied to the adsorbent used at the corresponding adsorption temperature. At 283 and 303 K, the methyl isobutyl ketone (MIBK) with higher polarity showed a better desorption of NCCs, while the degree of regeneration by methyl tertiary butyl ether (MTBE) at 323 K was the best. The adsorption of NCCs on the cogel was significantly affected by the presence of water in the LGO. While MTBE and MIBK effectively desorbed the adsorbed water with NCCs from the cogel, methyl phenyl ether (Anisole) with aromatic ring was not effective in treating the water. Since the adsorbent could select only the NCCs with high capacity from the LGO at mild temperature and ambient pressure, success in the adsorption technology process would lead to major advances in petroleum refining by facilitating the improvement of HDS as well as fuel cell applications by offering greater protection of the nitrogen-selective adsorbent. © 2005 American Institute of Chemical Engineers *AIChE J,* 52: 510–521, 2006
Keywords: denitrogenation, adsorption, desorption, light gas oil, logel

Introduction

Recently, since environmental problems from SO_x and NO_x in the combustion of fossil fuels became an object of public concern, refiners in most parts of the world are facing the inevitable reality that they will soon need to produce clean automotive fuels with ultra-low sulfur levels in the foreseeable future.

Despite the ever-tightening regulations of sulfur content, producing the currently acceptable 50 ppmw ULSD is already a considerable challenge for most refineries. Reducing the sulfur content of diesel fuel down to 10 ppmw or below will be an even greater challenge. At the moment, 10 ppmw ULSD is available only from a select few refiners that utilize conventional hydrodesulfurization (HDS) processes, under the condition that the sulfur content of virgin light gas oil

Correspondence concerning this article should be addressed to C.-H. Lee at leech@yonsei.ac.kr.

remains below 2,000-3,000 ppmw. However, in view of the tightening regulations and ongoing consumption of Earth's natural resources, much of the demand remains to be met with fuels from high sulfur light gas oil, which usually contains sulfur in the range of 8,000-15,000 ppmw.[1]

The HDS process is highly efficient in removing thiols, sulfides, and disulfides but is less effective for aromatic thiophenes and thiophene derivatives.[2] Moreover, alkylated dibenzothiophenes (DBTs) are the most difficult species to remove and make up most of the sulfur-containing compounds (SCCs), although refractory types make up only a small part of the total sulfur compounds.[3] This is because they have to compete with nitrogen compounds for active sites of catalysts for hydrogenation and because the nitrogen-containing compounds (NCCs) generally have higher adsorptivity compared to refractory compounds.[4] As a result, refractory SCCs are deprived of the chance to take up the active sites to be hydrogenated. Furthermore, since the denitrogenation reaction is slower than the desulfurization reaction, the NCCs' residue on the active sites remains longer than the SCCs, which also makes the refractory SCCs difficult to convert.[5] Therefore, removal of NCCs, especially basic nitrogen compounds, was conducted prior to hydrodesulfurization to facilitate the achievement of deep desulfurization using the conventional process.[5-7]

The new challenge is to use adsorption to selectively remove these sulfur and nitrogen compounds from transportation fuels regardless of the amount and types of sulfur compounds. All of the commercially available adsorbents and nonconventional adsorbents have been focused on desulfurization and have been proven ineffective.[8,9] Recently, Yang et al. reported that CuY zeolite can adsorb SCCs from commercial fuels (containing 430 ppmw sulfur) selectively and with high sulfur capacities at ambient temperature and pressure.[8] This adsorbent also simultaneously showed a high selectivity of NCCs in commercial diesel (containing 83 ppmw NCCs).[10]

However, even though the regeneration of the used adsorbent should be considered in achieving a cyclic adsorption process in bulk treatment, little research has been done on LGO. Thermal regeneration has been applied broadly as one of the methods among various other techniques for the regeneration of the spent adsorbents, but it has significant drawbacks in bulk processing, such as a high energy requirement, the production of air pollutants, a decrease in hardness of the adsorbent, and an enlargement in pore size. Instead, chemical regeneration of adsorbents using organic solvents might be a potential alternative to thermal regeneration due to its high regeneration rates as well as its effective recovery of the original integrity of the adsorbents.[11,12]

The purpose of this study was to achieve the denitrogenation of light gas oil (LGO) containing high SCCs by using Si-Zr cogel as an adsorbent. For this purpose, the adsorption equilibria and kinetics of NCCs in LGO on the Si-Zr cogel were measured at various feed compositions and temperatures. The desorption equilibria and kinetics of the NCCs using three kinds of solvents (MTBE, MIBK, and Anisole) were also studied at various feed compositions and temperatures. In addition, the re-adsorption of NCCs was compared with the silica-zirconia cogels regenerated by the three different solvents, taking into consideration the effect of water on the LGO. To investigate the validity of the continuous denitrogenation process of LGO, the adsorption and desorption dynamics of the Si-Zr cogel column were studied through the breakthrough and solvent regeneration experiments. These results will provide a valuable engineering database for the design of the adsorption process in the denitrogenation of LGO.

Table 1. Propertius of Adsorbents and Untreated LGO

Properties	Values	
	Zirconium-Free Silica Gel	Si-Zr Cogel
Type/Size [mesh]	Pellet/8	Pellet/16
BET surface area [m^2/g]	716	502
Bulk density [g/cm^3]	0.75	0.61
Pellet density [g/cm^3]	1.22	1.29
	Untreated LGO	
Distillation start point [K]	491	
10% distilled T [K]	524	
50% distilled T [K]	572	
90% distilled T [K]	618	
Distillation end point [K]	633	
Residues [vol %]	5	
Content of sulfur [ppmw]	8200	
Content of nitrogen [ppmw]	190	

Experimental Procedures

Materials

In this study, silica-zirconia (Si-Zr) cogel was used as an adsorbent, which was supplied by SK Co. (Korea) and Grace Davison Company (USA). For the purpose of comparison, a silica gel (Duksan Pure Chemicals Co., Ltd.) was also used. The properties of these adsorbents are listed in Table 1. The average particle size of the cogel was about 16 mesh, the pore size of the cogel was in the range of 63~67 Å, and the average pore diameter was 66 Å. From the XPS spectrum (ESCALAB 220I-XL, Fisons Co.) of Si-Zr cogel, Zr^{4+} was found at the Zr3d band, and the amount of Zr in the Si-Zr cogel was about 3%. The average particle size of the zirconium-free silica gel was about 8 mesh, and the average pore diameter was 120 Å.

The two types of light gas oils (LGOs) were supplied by SK Co. One was an untreated LGO containing NCCs of about 190 ppmw and SCCs of about 8,200 ppmw. The treated LGO was prepared by removing about 90% of the NCCs from the untreated LGO using the denitrogenation step. The boiling point range of the untreated LGO is presented in Table 1. To prepare the treated LGO, the untreated LGO passed several times through the Si-Zr cogel bed at 313K. Then, kerosene was used to make the same density with the untreated LGO. The treated LGO contained NCCs of 20 ppmw, but the concentration of SCCs was the same as the untreated LGO, about 8200 ppmw.

LGOs are composed of several thousand kinds of hydrocarbon compounds. The main components among these can be classified into three types: sulfur-containing compounds (SCCs), nitrogen-containing compounds (NCCs), and oxygen-containing compounds (OCCs). Representative SCCs are dimethylthiophene, 4-methyldibenzothiophene, 4,6-dimenthyldibenzothiophene, 3C-dibenzothiophene, and 3C-dibenzothiophene. Representative NCCs are pyridines, tetrahydroquinolines, quinolines, acridines, indoles, carbazoles, and benzocarbazoles. Representative OCCs are phenols and dibenzofuran. The nitrogen chromatogram of the untreated LGO was measured using GC-AED, as shown in Figure 1. It identified 29 carbazoles: mono-, di-, and trimethyl-carbazoles, as major components of the untreated LGO.

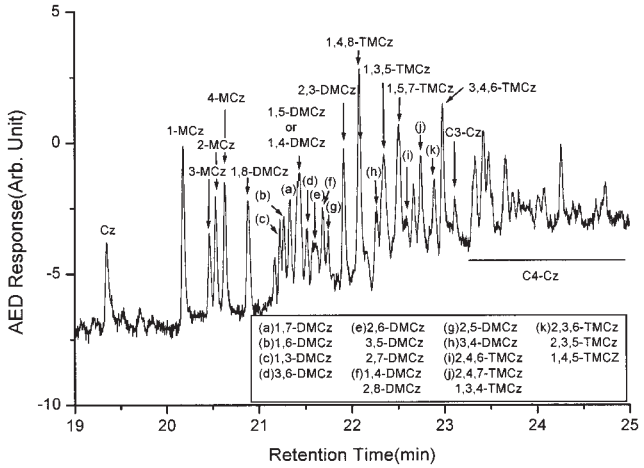

Figure 1. GC-AED nitrogen chromatogram of untreated LGO.

In this study, the adsorbent used was regenerated by three different solvents. The solvents selected as desorbents were MTBE (Acros Organics, 99%), MIBK (MIBK; Junsei Chemical Co., +99.5%), and Anisole (Junsei Chemical Co., +98%). These solvents have different polarities, boiling points, and solvent capabilities for NCCs. The properties of these solvents are presented in Table 2.

In the batch experiments, the vial bottle with 12mL volume was used and the concentration gradient in the bottle was assumed to be negligible. The concentrations of NCCs and SCCs were measured by an N-S analyzer (ANTEK, 9000 series). The standard component for the SCCs was dibenzothiophene (DBT), while for the NCCs it was 9-methyl carbazole. Toluene (Duksan Pure Chemical Co. Ltd., +99.5%) was selected as the base component for calibration. In the adsorption and desorption experiments, 10 μL was sampled from the solution sample each time.

Adsorption equilibria and kinetics

The batch adsorption method was used to determine the adsorption equilibrium and kinetics. A circulator (Jeio Tech) and a chiller (FTS systems Inc.) were used to maintain the constant temperature of the vial bottles.

The LGO mixtures at several volume ratios (treated LGO : untreated LGO), 10 : 0~0 : 10, were prepared in 11 vial bottles, which correspond to samples 1 to 11 in Table 3. The volume of each LGO mixture was about 10 mL. Before each experiment, about 100 mg of adsorbent was regenerated in an open vial bottle at 423 K for 10 h. Then, the amount of adsorbent was re-measured in the sealed condition to prevent adsorption of water from air. The activated adsorbent was mixed with an LGO sample for more than 3 d until it reached equilibrium. The amounts of NCCs and SCCs in the LGO sample before and after adsorption equilibrium were analyzed using the N-S analyzer. On the other hand, the adsorption kinetics of the LGO mixture were obtained by the transient amounts of NCCs in the LGO mixture until equilibrium was reached. The adsorption equilibria and kinetics of the LGO samples on Si-Zr cogel were measured at 283, 303, and 323 K. The schematics of the experimental procedure is shown in Figure 2a.

Table 3. Concentrations of NCCs and SCCs at Several Volume Ratios of Treated and Untreated LGOs

LGO Mixtures	Volume Ratio (treated:untreated)	Concentrations of NCCs [ppmw]	Concentrations of SCCs [ppmw]
Sample 1	10:0	19.9	
Sample 2	9:1	36.7	
Sample 3	8:2	53.5	
Sample 4	7:3	70.3	
Sample 5	6:4	87.1	
Sample 6	5:5	103.9	8200
Sample 7	4:6	120.8	
Sample 8	3:7	137.6	
Sample 9	2:8	154.4	
Sample 10	1:9	171.2	
Sample 11	0:10	188.0	

Desorption equilibria and kinetics

The Si-Zr cogels used in the adsorption equilibria and kinetics were applied for the measurements of desorption equilibria and kinetics. At each desorption experiment, the same amount of LGO (9.5 mL) was removed by a 10mL syringe from the vial that had been used for the adsorption equilibrium experiments. The vial was reweighed to confirm the amount of LGO from the known weights of vial and adsorbent. Then, to obtain desorption equilibria and kinetics, three kind of solvents used as desorbents were added into the above bottles, which contained Si-Zr cogels with the LGO residue. The wetted adsorbent with the LGO was soaked in each solvent for more than 3 d until it reached equilibrium. In the desorption experiment using MTBE, MIBK, and Anisole, the desorption temperature was applied to the adsorbent used at the corresponding adsorption temperature.

Re-Adsorption

For the re-adsorption experiments, the cogels that had once been adsorbed by the LGO and then desorbed by the solvents

Table 2. Properties of Solvents[13]

Properties	MTBE (Methyl tertiary butyl ether)	MIBK (Methyl isobutyl ketone)	Anisole (Methylphenyl ether)
Formula	$(CH_3)_3 \cdot COCH_3$	$(CH_3)_2CHCH_2 \cdot COCH_3$	$C_6H_5OCH_3$
Molecular weight [−]	88.15	100.16	108.14
Dipole moment [debyes]	1.2	2.8	1.2
Acentric factor [−]	0.269	0.385	0.347
Melting point [K]		189	235.7
Boiling point [K]	328.3	389.6	426.8
Density [g/cm^3]	0.740 (293.15 K)	0.80 (293.15 K)	0.996 (293.15 K)

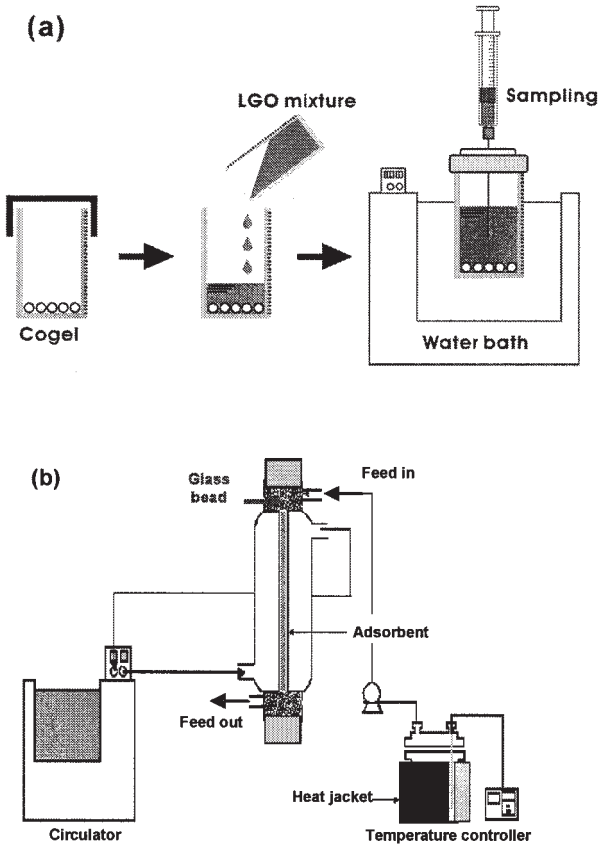

Figure 2. (a) Experimental procedure for equilibrium and kinetics, and (b) schematic diagram of dynamic apparatus.

were used. Prior to each re-adsorption experiment, the same amount of the residual liquid (9.5 mL) was removed by a 10mL syringe from the vial used in the desorption experiment. After measuring the mass of regenerated adsorbents wetted by each solvent (MTBE, MIBK, and Anisole), the re-adsorption experiments in the vial with the wetted adsorbent were performed at the corresponding desorption temperature of 283, 303, and 323 K.

Effect of water

The LGO sometimes contains a certain amount of water from previous stage processes. To investigate the effect of water on the cogel, the adsorption and desorption of LGO were measured using water-saturated LGO. In preparing the water-saturated LGO, ultra-pure water (J. T. Baker, HPLC grade) was mixed with the untreated LGO sample (sample 11) and agitated in the bottle for a sufficient time at 303 K. After phase separation, the water-saturated LGO was used for the experiments.

The following procedure was performed to observe the effect of water: First, the three samples of activated Si-Zr cogel were prepared. Then, the adsorption equilibria of the water-saturated LGO were measured in the three samples. Following that, each sample in wetted condition was desorbed by MTBE, MIBK, and Anisole, respectively. Finally, each sample at the wetted condition was re-adsorbed by the water-free untreated LGO. In the experiments, the temperature was fixed at 303 K.

Adsorption and desorption dynamics

Figure 2b shows the schematic diagram of the equipment for the dynamic experiments. The adsorption bed was made of glass with 6.5 cm length and 0.7 cm ID, and the amount of Si-Zr cogel in the adsorption bed was 1.515 g. After the activated adsorbents were packed in the bed, a sieve was inserted at each end of the adsorbent to prevent the loss of adsorbents. Then, each end of the bed was packed with glass beads to minimize end effect. To maintain the constant temperature of the bed, a thermostat circulator was used.

In the adsorption and desorption experiments, the LGO mixture or solvent was supplied to the bed by a solvent delivery pump (Sodine Electronic Company, NYC-13D3) through the preheater. The effluents from the bed were sampled at a proper time interval and were analyzed with the N-S analyzer. The adsorption experiments were performed in the range of 303~323 K and 0.5~1.5 ml/min. Then, the desorption experiments were conducted at a fixed flow rate and temperature of 1.3 ml/min and 303 K, respectively. Additionally, re-adsorption dynamics were analyzed at 303 and 323 K, respectively, at a fixed flow rate of 1.0 ml/min. The desorption and re-adsorption experiments were performed in a wetted condition like the above batch experiments.

Results and Discussion

The density changes of the LGO samples at various volume ratios (samples 2-7) were measured along with the temperatures, as shown in Figure 3. As shown in Figure 3, density was nearly constant irrespective of the volume ratio. However, density was linearly reduced from 0.85 to 0.80 g/cm^3 as temperature increased from 283 to 363 K. This result will be used for the explanation of the temperature dependence of the equilibrium and kinetic parameters.

Table 4 shows the changes in the concentrations of NCCs and SCCs before and after the adsorption equilibria on the

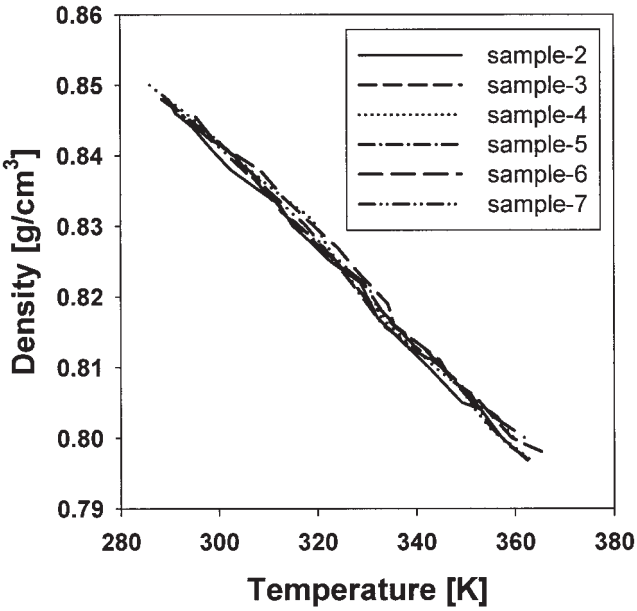

Figure 3. Density change of several LGO samples with temperature.

Table 4. Changes in the Concentrations of NCCs and SCCs Before and After the Adsorption Equilibria on Co-Gel for Each Sample at 303 K

LGO Mixtures	Concentrations of NCCs [ppmw]	Concentrations of SCCs [ppmw]
Sample 1	19.9 → 13.0	8200 → 8207
Sample 2	36.7 → 19.2	8200 → 8227
Sample 3	53.5 → 28.7	8200 → 8219
Sample 4	70.3 → 37.8	8200 → 8218
Sample 5	87.1 → 55.2	8200 → 8263
Sample 6	103.9 → 68.4	8200 → 8225
Sample 7	120.8 → 80.4	8200 → 8234
Sample 8	137.6 → 99.5	8200 → 8261
Sample 9	154.4 → 112.8	8200 → 8276
Sample 10	171.2 → 127.9	8200 → 8232
Sample 11	188.0 → 148.1	8200 → 8251

cogel for each LGO sample at 303 K. The amount of the adsorbent applied was slightly different in each experiment because the amount of activated adsorbent was measured in a sealed bottle to prevent water adsorption from air. Since the concentration of SCCs was measured at the high concentration range of the analyzer, the results were scattered within less than 1% of a full range. As shown in Table 4, the concentration of NCCs in each sample remarkably decreased after adsorption equilibrium while change was negligible in the concentrations of SCCs. This implies that the Si-Zr cogel adsorbent only has selectivity for the NCCs in the LGO. In addition, the SCCs in the LGO can be considered as inert in the experiments, although the concentration of SCCs is much higher than that of the NCCs. In this study, the NCCs were considered a pseudo-single component. Therefore, the LGO was considered a pseudo-binary system although it consists of several thousand components.

Adsorption equilibria and kinetics of NCCs

The adsorption isotherms of NCCs on the cogel at 283, 303, and 323 K are shown in Figure 4. All the isotherms were favorable in Type I. The adsorbed amount steeply increased in the low concentration range, and then slowly increased as the concentration increased. All the isotherms were fitted using the following Langmuir model, and the isotherm parameters are listed in Table 5

$$C_\mu = C_{\mu s} \cdot \frac{b \cdot C}{1 + b \cdot C} \tag{1}$$

It is noteworthy that the temperature dependency of the isotherms was different from the general adsorption phenomena, which is generally an exothermic process. In this study, the adsorbed amount of NCCs increased as temperature increased from 283 to 323 K. Another interesting phenomenon in the isotherms was observed between 303 K and 323 K. As the temperature changed from 283 K to 303 K, the difference between the adsorbed amounts at each of the two temperatures became approximately parallel in the whole range of the experimental NCCs concentration. However, in the case of 303 and 323 K, the adsorbed amount of NCCs was almost the same as the range of low NCC concentration. Furthermore, the difference in the adsorbed amount between each of the temperatures increased gradually with an increase in the concentration of NCCs. Hence, under high NCC concentration conditions, the difference in the adsorbed amounts between 303 and 323 K was much higher than that between 283 and 303 K.

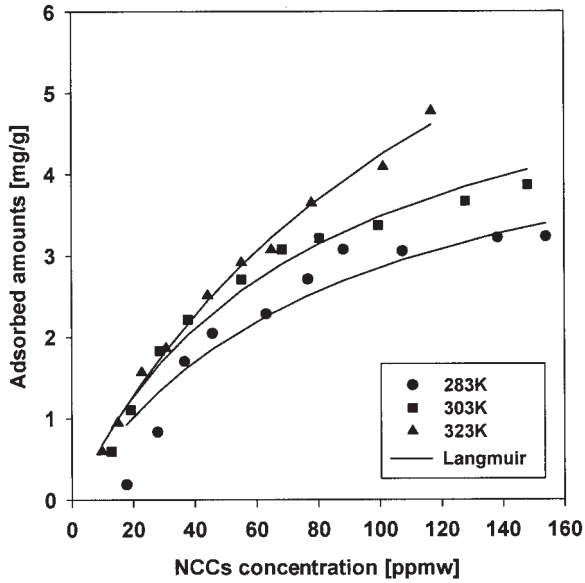

Figure 4. Adsorption isotherms of NCCs on Si-Zr cogel at 283, 303, and 323 K.

The adsorbed amounts of NCCs on the Si-Zr cogel and silica gel at 323 K are compared in Figure 5. The Si-Zr cogel showed about four times the adsorbed amount of the silica gel regardless of surface area (Table 1). This implies that the zirconia of the cogel plays a key role in improving the adsorption and selectivity of NCCs in the LGO.

The uptake experiments for adsorption were performed under static conditions without any mixing. Figure 6 shows the uptake curves for the NCCs adsorption of untreated LGO (sample 11) on the cogel at 283, 303, and 323K, respectively. In this study, it was hard to predict the accurate adsorption mechanism with a specific model because the NCCs are composed of various components. Nevertheless, under the assumption that the micropore diffusion is a rate-limiting mechanism in the NCCs/Cogel adsorption system, the following Fickian diffusion model was applied to extract "pseudo" diffusional time constants from the non-linear regressions of uptake curves using a Nelder-Meader optimizer.[14]

$$F = 1 - \frac{6}{\pi^2} \sum_{n=1}^{\infty} \frac{1}{n^2} \exp\left(\frac{-n^2 \pi^2 D_e t}{R_p^2}\right) \tag{2}$$

Table 5. Langmuir Isotherm Parameters for NCCs Adsorption on Si-Zr Cogel

Temp. [K]	$C_{\mu s}$ [mg/g]	b [1/ppmw]
283	5.2340	0.0120
303	6.1740	0.0129
323	10.018	0.0073

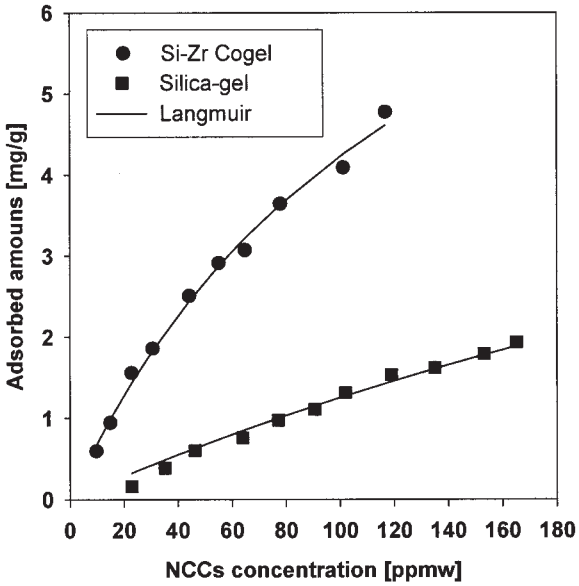

Figure 5. Comparison of adsorbed amount for Si-Zr cogel and silica-gel at 323 K.

Here, F represents the fractional uptake, and D_e/R_p^2 the pseudo-diffusional time constant.

The pseudo-diffusional time constants (D_e/R_p^2) at three temperatures are presented in Table 6. Although these values include the assumptions, it is helpful to understand the kinetic characteristics of NCCs by a relative comparison of each other. In comparison with 323 K, it took a much longer time to approach adsorption equilibrium at 283 and 303 K. On the other hand, the difference in the time taken to reach the adsorption equilibrium at 283 and 303 K was small, although the diffusional rate at 303 K was faster than that at 283 K. In effect, when the temperature was increased, the adsorption rate

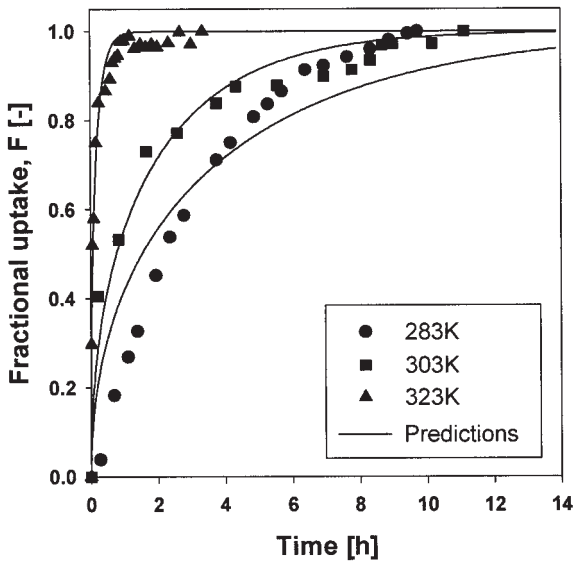

Figure 6. Uptake curves of untreated LGO on Si-Zr cogel at 283, 303, and 323 K.

Table 6. The Pseudo-Diffusional Time Constants for the Adsorption and Desorption Uptake

	D_e/R_p^2 [10^{-4} s^{-1}]			
		Desorption		
Temp. [K]	Adsorption	MTBE	MIBK	Anisole
283	0.056	—	—	—
303	0.11	0.30	0.16	0.22
323	1.3	0.46	0.76	1.5

as well as the adsorption amount was improved simultaneously.

These phenomena of adsorption equilibrium and kinetics lead to the following postulations: (1) Since the molecules of NCCs would be activated with an increase in temperature, relatively large molecules among the NCCs could pass through the pore entrance easily. As shown in Figure 3, the density of the LGO sample was linearly decreased with an increase in temperature even though the variation was small. (2) Since the zirconia of Si-Zr cogel would be more active as the temperature increased, a greater amount of NCCs could be readily adsorbed on the surface. And the activated zirconia may induce strong interactions between the adsorbent surface and the adsorbate or among the adsorbates themselves even though the increase in temperature is small. These postulations will be discussed further along with the results of desorption equilibria and kinetics.

Effects of solvent on desorption equilibria and kinetics

The NCCs adsorbed on Si-Zr cogel were desorbed by three solvents: MTBE, MIBK, and Anisole. As mentioned in the Experimental section, the adsorbent used at a specified temperature for the adsorption experiment was also used in the desorption experiment at the same corresponding temperature.

In this study, the regeneration ability of each solvent was expressed as a desorption ratio, defined as follows

$$\textit{Desorption ratio} = \frac{\textit{Desorbed amounts}}{\textit{Adsorbed amounts before desorption}} \quad (3)$$

Figures 7a to 7c show the regeneration ability of each solvent at three temperatures. In each of the cases of MTBE, MIBK, and Anisole, the desorption ratio was smaller at higher temperatures than at lower temperatures. As shown in Figure 7a, the average desorption ratio of MTBE under each temperature did not show a significant deviation in the whole concentration range. This implies that the desorption ratio was hardly affected by the adsorbed amounts in the case of MTBE. Similar to MTBE, the desorption ratio of Anisole under each condition showed a somewhat linear relationship at each of the temperatures in the whole concentration range. However, in the case of MIBK (Figure 7b), the desorption behavior was different from MTBE and Anisole. The average desorption ratios at 283 and 303K did not show a significant deviation in the whole concentration range. On the other hand, at 323 K, the average desorption ratio was 65.20% in the case of the adsorbent adsorbed at the range of low NCC concentration (Figure 4). Following that, the desorption ratio steadily decreased to 38%

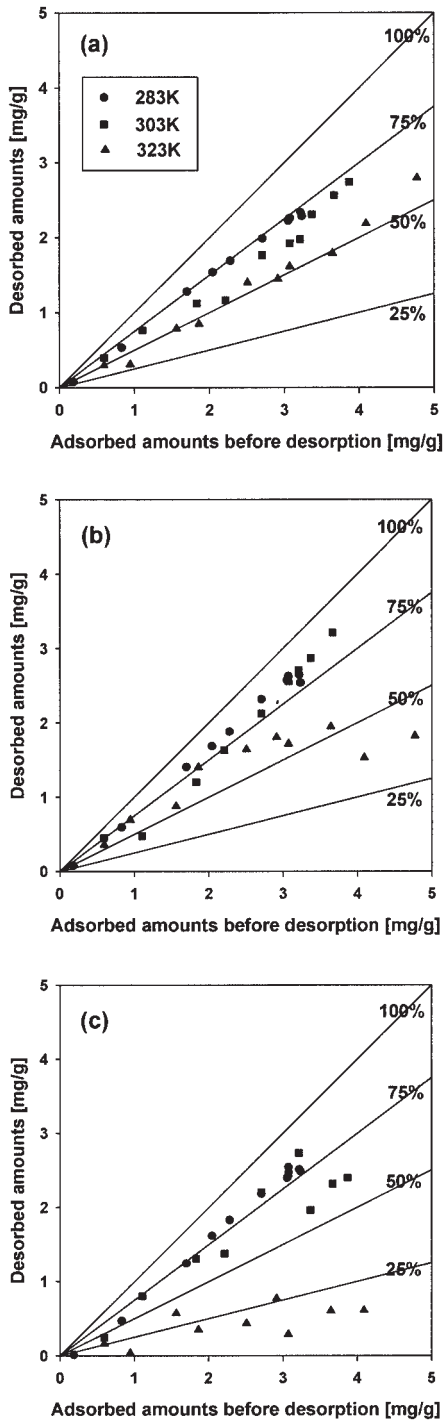

Figure 7. Regeneration abilities of (a) MTBE, (b) MIBK, and (c) Anisole at 283, 303, and 323 K.

and remained constant even though the adsorbed amount increased. This means that the desorption amount at 323 K remained almost constant in the case of the adsorbent adsorbed at high concentration range regardless of the adsorbed amount shown in Figure 4.

Even though desorption is an endothermic mechanism, it has clearly been shown that the desorption amount and desorption ratio are not dependent upon applied temperature (Figure 7). At 283 and 303 K, the desorption abilities of all the solvents maintain the order of MIBK > Anisole > MTBE in the whole concentration region. The result implies that high polar solvent (MIBK in this study) works better to desorb the NCCs on the Si-Zr cogel that were adsorbed at these temperatures. In the case of solvents with similar polarity (MTBE and Anisole), the solvent with aromatic ring (Anisole) demonstrated a better regeneration ability at each of the two temperature conditions. However, at 323 K, MIBK showed the highest regeneration ability in the low concentration region while MTBE was the best solvent in the high concentration region. On the other hand, Anisole demonstrated much lower regeneration ability than the other solvents at 323 K. Therefore, this suggests that the polarity and aromatic functional group of solvents hardly contribute to improving the desorption of NCCs adsorbed at 323 K, a different effect than that which results from the other two temperatures.

The NCCs in the LGO consist of two groups: One is a strong basic group with a pyridine ring, such as pyridines, tetrahydroquinolines, quinolines, acridines, etc. The other is a weak acidic group with a pyrole ring, such as indoles, carbazoles, benzocarbazoles, etc. Morterra et al. reported that the vacuum thermal activation of microcrystalline monoclinic ZrO_2 in the 25-600°C range causes the gradual elimination of the surface hydrated layer.[15] This layer is made up of hydroxyl species, and its vacuum thermal elimination brings about the formation of several families of surface Lewis acid sites (coordinatively unsaturated Zr^{+4} ions), capable of coordinating various Lewis bases at ambient temperature. In addition, it has been proven that the incorporation of zirconium into a silica framework provokes a linear increase of both the Lewis and Brønsted acidities by the adsorption of basic molecules, such as pivalonitrile and pyridins.[16] From Figure 7 then, it can be expected that the Si-Zr cogel at 323 K should show a selectivity of specific components among the NCCs with a strong affinity as detailed in the above postulations. In addition, such phenomena are consistent with the results of adsorption equilibria and kinetics in Figures 4 and 6.

Figures 8a to 8c show the desorption uptake curves of the pre-adsorbed Si-Zr cogels (sample 11) at 303 and 323 K in a batch system. The pseudo-desorption diffusional time constants predicted by the Fickian diffusion model (Eq. 2) are summarized in Table 6. In this study, the desorption kinetics could not be measured at 283 K because phase separations between NCCs and solvents were observed. In the regeneration experiments by each solvent, the desorption rate at 323 K was faster than that at 303 K, while the desorption rate of each solvent was not significantly different at 303 K. This is because the desorbed amount at 323K was smaller than that at 303K, and the desorbed amount by each solvent was not significantly different at 303K, as shown in Figure 7. Compared with the results of MIBK and Anisole, the difference between the two temperatures in the desorption rate of MTBE was relatively small because the difference between the desorbed amounts at the two temperatures was relatively small. As reported in Table 6, the desorption rates of MIBK and Anisole at 323K were two and three times faster than that of MTBE, respectively, because the relative desorbed amounts by these two solvents were much smaller than that by MTBE at 323K. It can be inferred from Figure 7 that MTBE takes more time than MIBK and Anisole to desorb the adsorbed NCCs, which include some parts of the

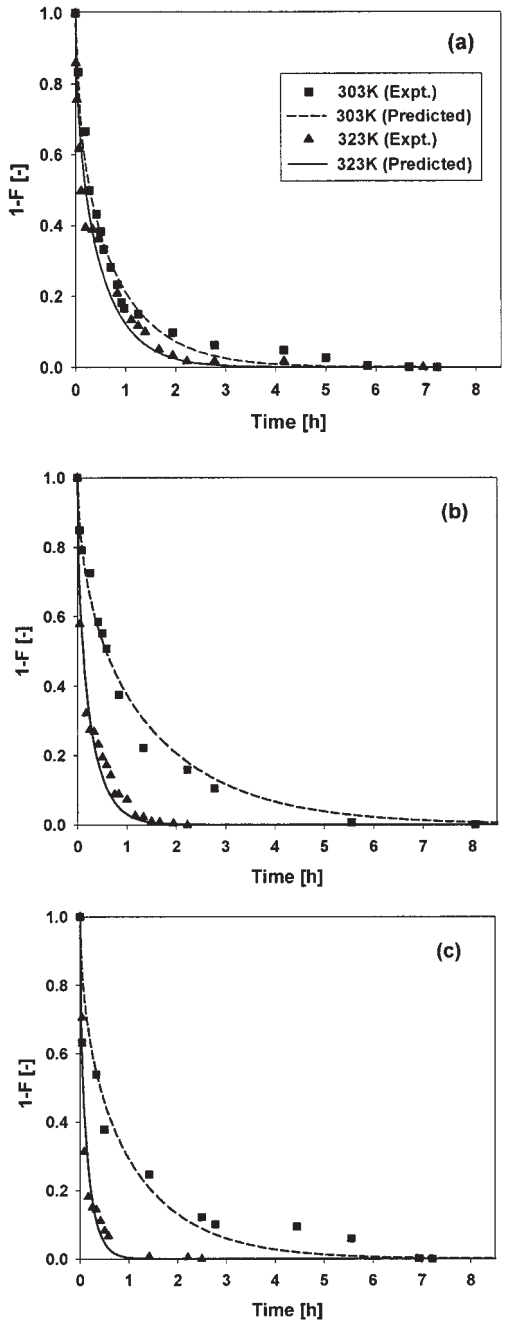

Figure 8. Desorption uptake curves by (a) MTBE, (b) MIBK, and (c) Anisole as a solvent.

strong adsorbates. On the other hand, MIBK with strong polarity and Anisole with an aromatic ring seem to desorb the weak adsorbates easily at high temperatures. In addition, the higher desorption temperature seems to enhance the movement of these two solvents, which are relatively larger than MTBE.

Re-Adsorption ability of solvent-regenerated cogel

In this study, re-adsorption ability was measured using the cogel that was regenerated by the solvents under each of the conditions (Figure 7). Figures 9a to 9c show the re-adsorption abilities when MTBE, MIBK, and Anisole were used as solvents, respectively. In each Figure, the re-adsorbed amounts at each of the temperatures are compared with the adsorption isotherms of the virgin cogel in Figure 4. Notwithstanding a decrease in re-adsorption ability (Figure 9), the re-adsorption amount of the cogel regenerated by MTBE and Anisole at 323 K was smaller than at 283 and 303 K. In the case of Anisole especially, the re-adsorption amount at 323 K was very small.

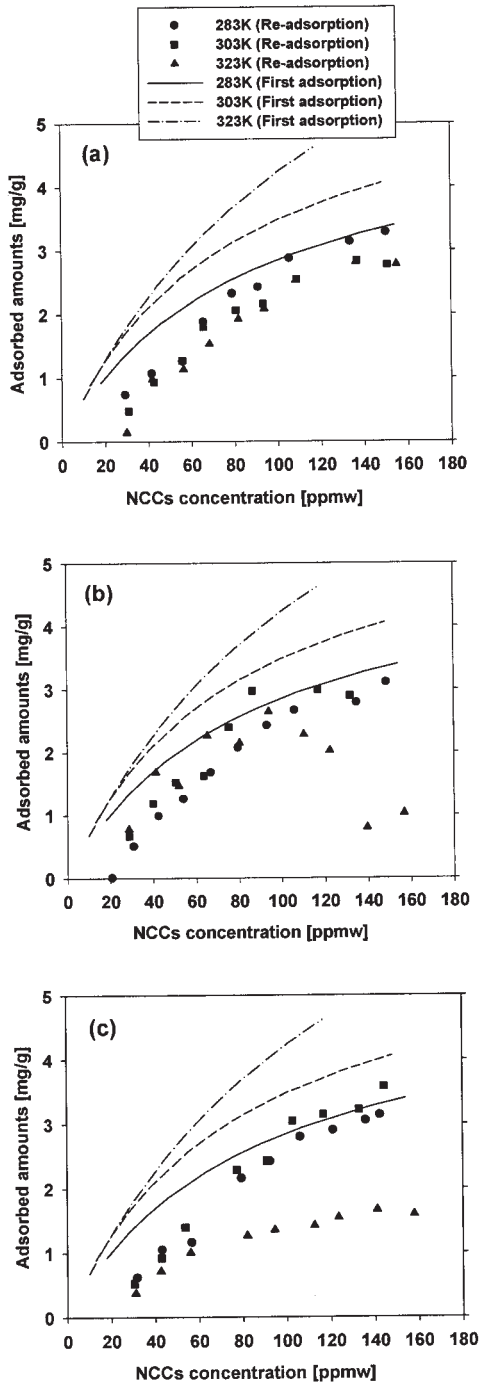

Figure 9. Re-Adsorption isotherms of NCCs on Si-Zr cogel at 283, 303, and 323 K; the adsorbent was regenerated by (a) MTBE, (b) MIBK, and (c) Anisole as a desorbent.

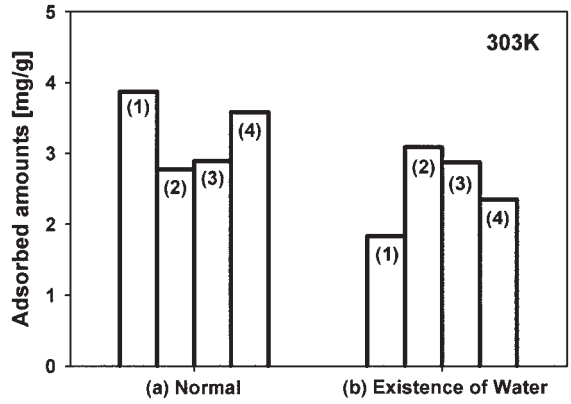

Figure 10. Effect of water on the adsorption and re-adsorption of NCCs on Si-Zr cogel at 303 K.

(a) Normal case: (1) Adsorbed amount of water-free LGO (sample 11), (2)~(3) Re-Adsorbed amounts of water-free LGO (sample 11) after the desorption by MTBE, MIBK, and Anisole, respectively.

(b) Existence of water in LGO: (1) Adsorbed amount of water-saturated LGO, (2)~(3) Re-Adsorbed amounts of water-free LGO (sample 11) after the desorption by MTBE, MIBK, and Anisole, respectively.

With MIBK, the re-adsorption amount at 283 K was smaller than that at 303 and 323 K, in the range of less than 90 ppmw NCCs (Figure 9b). However, the re-adsorption ability at 323 K decreased steeply from above 90 ppmw NCCs. These clearly stemmed from the degree of desorption in Figures 7a to 7c, not from any exothermic adsorption. The conclusion can be drawn, then, that the cogel will show a selective preference for specific groups of NCCs with an increase in adsorption temperature. Moreover, it can be deduced that the basic group of NCCs acts as the strong adsorbates on the surface Lewis acid sites, although, as shown in Figure 1, weak acidic carbazoles are the dominant NCCs in the feed.

Effects of water on adsorption and re-adsorption

In actual industrial fields, it is possible that the LGO, produced through various processes, could include a small amount of water. In this study, to investigate the effect of water on the NCC adsorption of cogel, the adsorption and re-adsorption of the NCCs was measured using the water-saturated LGO.

Figure 10 compares the adsorption and re-adsorption abilities of water-free LGO with water-saturated LGO at 303 K. In Figure 10a, the results of the normal case using water-free LGO (sample 11) were taken from Figure 9. At 303 K, the order of the re-adsorbed amount was desorption by Ansiole (4) > desorption by MIBK (3) > desorption by MTBE, (2) showing smaller adsorption amount than the first-adsorbed amount (1).

On the other hand, as shown in Figure 10b, the first-adsorbed amount in the water-saturated LGO was highly decreased by the presence of water in the LGO. It can be inferred that hydroxyl groups on the surface of Si-Zr cogel could play a role in the water adsorption. That is, since the hydroxyl group on the surface of Si-Zr cogel might adsorb water onto the surface through dispersion and polar forces,[17] the physically adsorbed water could be considered to inhibit the adsorption of NCCs on the Si-Zr cogel (Figure 10b). After being regenerated by the solvents, the re-adsorbed amounts in the water-free LGO were quantifiably larger than the first-adsorbed amounts because the water was effectively removed by the solvents. The order of the re-adsorbed amount at 303K was desorption by MTBE (2) > desorption by MIBK (3) > desorption by Anisole (4). When the re-adsorbed amounts in both cases (Figures 10a and 10b) were compared, the re-adsorption amounts of the cogel affected by water were slightly larger than those of the normal case in MTBE and MIBK. It is possible that the NCCs can be adsorbed on the water occupied sites desorbed by these solvents. On the other hand, Anisole is not recommended to treat the water on the cogel.

Adsorption and desorption dynamics

Since the equilibria and kinetics of adsorption and desorption were studied in a static-batch system without any mixing, the breakthrough experiments of the untreated LGO (sample 11) were conducted to obtain information on the dynamics of the bed.

Figures 11a and 11b show the effects of temperature and flow rate on the adsorption breakthrough curves using the untreated LGO (sample 11) in the Si-Zr cogel packing bed. Since the cogel demonstrated a larger adsorption capacity at 323 K (Figure 4), the breakthrough time was slower than at 303 K (Figure 11a). However, the tailing of the breakthrough curve was prominent at both temperatures. In Figure 11b, the tailing of the breakthrough curve became prominent as the flow rate decreased. Under 0.5 ml/min especially, the breakthrough curve reached steady state very slowly. From Figure 11b, it can be observed that the adsorption of NCCs on the cogel is affected by kinetic as well as equilibrium effects. When the contact time between liquid and solid phases grows longer, most of the active sites in the bed, including large molecules, can be adsorbed by the NCCs.

Figures 12a and 12b show the desorption dynamics of the bed that had been adsorbed at 303 and 323 K, respectively. In the experiments, the flow rate and temperature of the solvent were fixed at 1.3 ml/min and 303 K, respectively. Compared with the adsorption breakthrough curves in Figure 11, the desorption curves reached a steady state much more quickly. As shown in Figure 12a, the order of the desorption amount and rate at 303 K were as follows: MIBK > MTBE > Anisole. The difference in desorption between MIBK and MTBE can be explained by the regeneration ability of the solvent in the high concentration region at 303 K, as shown in Figure 7. On the other hand, although the regeneration ability of Anisole was similar to MTBE (even higher) at this condition, poor desorption behavior was observed in the desorption breakthrough curve. This implies that the kinetic effect played a key role in the desorption dynamics like the adsorption dynamics in the case of Anisole with an aromatic ring. When the adsorption temperature was 323 K, the desorption amounts of MTBE and Anisole became larger while that of MIBK was similar to the result at 303 K.

Figures 13a and 13b show the re-adsorption breakthrough curves in the Si-Zr cogel bed regenerated by each solvent at 303 and 323 K, respectively. In all the measurements, the flow rate was fixed at 1.0 ml/min. In Figure 13a, the breakthrough times in the MIBK and Anisole regeneration cases were similar to each other, while that of the MTBE case lagged slightly

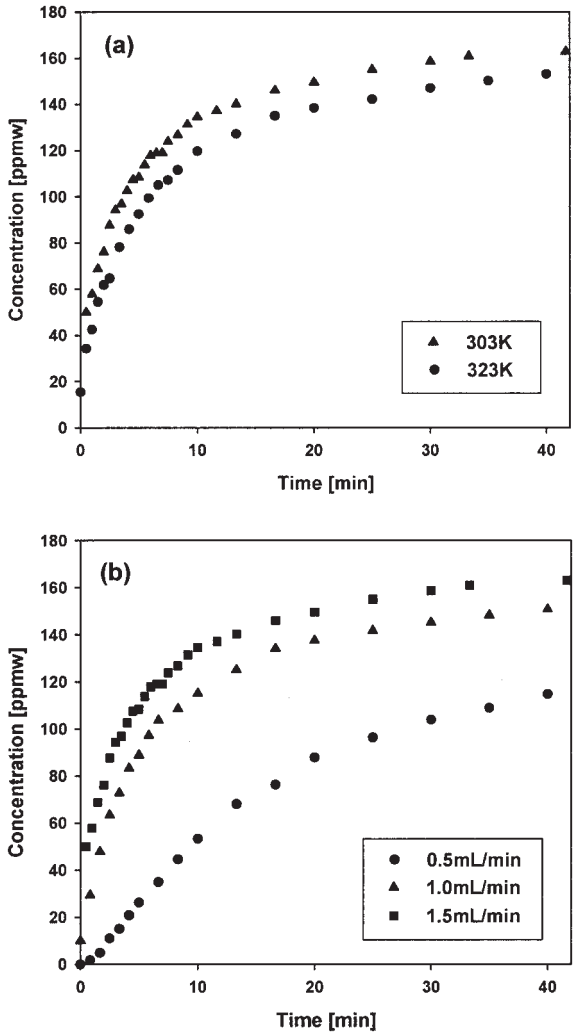

Figure 11. Adsorption breakthrough curves by using sample 11.

(a) Effect of temperature (flow rate = 1.5 ml/min), and (b) Effect of flow rate (at 303 K).

behind those of the others. However, as expected of the desorption amount of MIBK (Figure 12a), the breakthrough curve in the case of MIBK shows prominent tailing. In Figure 13b, the breakthrough time of each solvent followed the order of MTBE > MIBK > Anisole, although the desorption performances of MTBE and MIBK were similar to each other in Figure 12b. This implies that, as expected in Figures 7 to 9, the regeneration ability of MIBK for specific components in the NCCs was worse than that of MTBE.

Figure 14 shows an example of the cyclic operation of the denitrogenation of the LGO consisting of the three steps (adsorption, solvent desorption, and re-adsorption). When the cycle was operated using sample 11 and MTBE at 303 K, the desorption step-time was enough for approximately half the adsorption step-time. Furthermore, a certain amount of the NCCs was successfully removed from LGO through the solvent swing adsorption process. Work is currently underway to optimize the adsorptive denitrogenation of LGO in the multiple cyclic process.

Conclusions

The characteristics of adsorption and desorption of NCCs on the Si-Zr cogel were studied for a denitrogenation of the LGO containing a high concentration of SCCs. The Si-Zr cogel adsorbent demonstrated a selective preference only for NCCs regardless of the amount and types of SCCs in the LGO because the zirconia of the cogel played a key role in improving the adsorption and selectivity of NCCs in the LGO.

The adsorbed amount of NCCs increased as temperature increased from 283 to 323 K even though adsorption is generally an exothermic process. Furthermore, the time taken to reach adsorption equilibrium at 323 K was shorter than at 303 K. On the other hand, even though desorption is an endothermic mechanism, it has clearly been demonstrated that the regeneration ability of the solvent becomes worse at higher temperature when the desorption temperature is applied to the adsorbent at the corresponding adsorption temperature. The desorption abilities of all the solvents varied with temperature

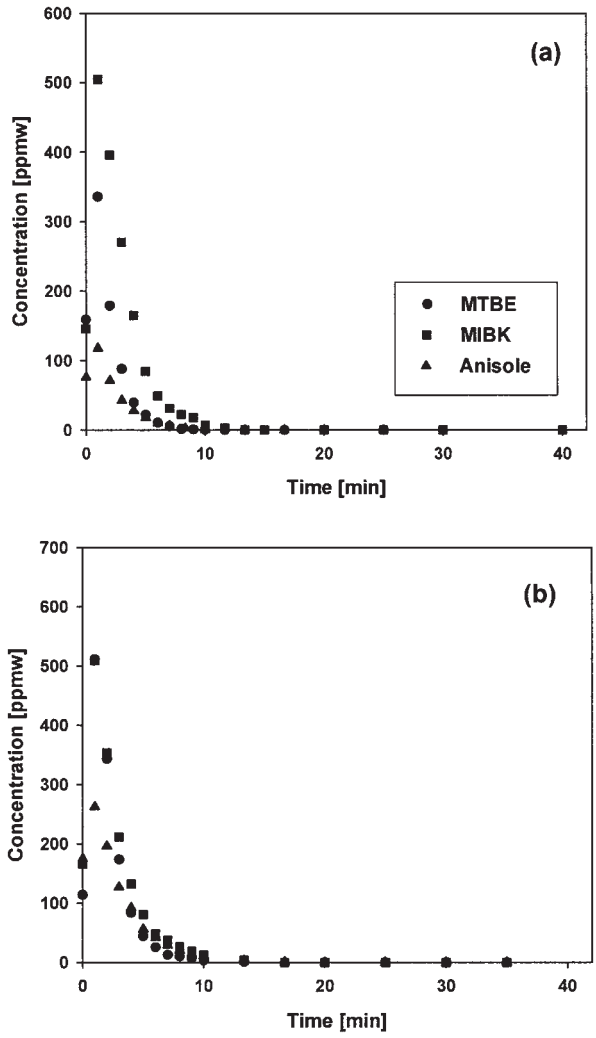

Figure 12. Effect of desorbent on the extraction curves for the beds that had been adsorbed at (a) 303 K and (b) 323 K, respectively (desorption condition: flow rate = 1.3 ml/min, temperature = 303 K).

and NCCs concentration. Also, re-adsorption ability was found to be deeply related to the degree of desorption of each solvent.

The adsorbed amount of NCCs on the cogel was significantly decreased by the presence of water in LGO, because the physically adsorbed water might inhibit the adsorption of NCCs on the Si-Zr cogel. While MTBE and MIBK effectively desorbed the adsorbed water with NCCs from the cogel, Anisole is not recommended to treat the water.

From the dynamic experiments in the bed, it is clearly shown that the adsorption and desorption behaviors of NCCs on the cogel were significantly affected by kinetic as well as equilibrium effects. The adsorption of relatively large molecules or certain strong adsorbates in the NCCs seemed to be affected by kinetic hindrance. Since the adsorbed species of the NCCs depended heavily on applied temperature, the operating temperature had to be determined with careful consideration to remove targeted compounds of the NCCs. In addition, the choice of solvents strongly depended on the applied temperature rather than their physical properties.

Since the adsorbent could select only the NCCs from the LGO and adsorption and desorption could be accomplished at mild temperatures and ambient pressure, success in adsorption technology would lead to major advances in petroleum refining by effecting the improvement of HDS as well as fuel cell applications through the protection of nitrogen-selective adsorbent.

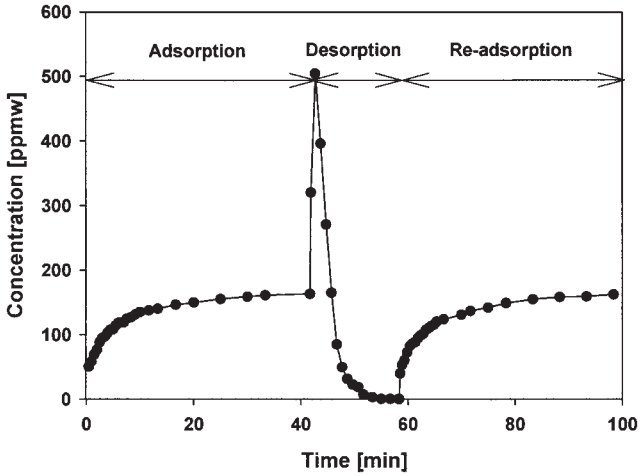

Figure 14. Cyclic operation by using sample 11 and MTBE at 303 K, 1.0 ml/min (adsorption), and 1.3 ml/min (desorption).

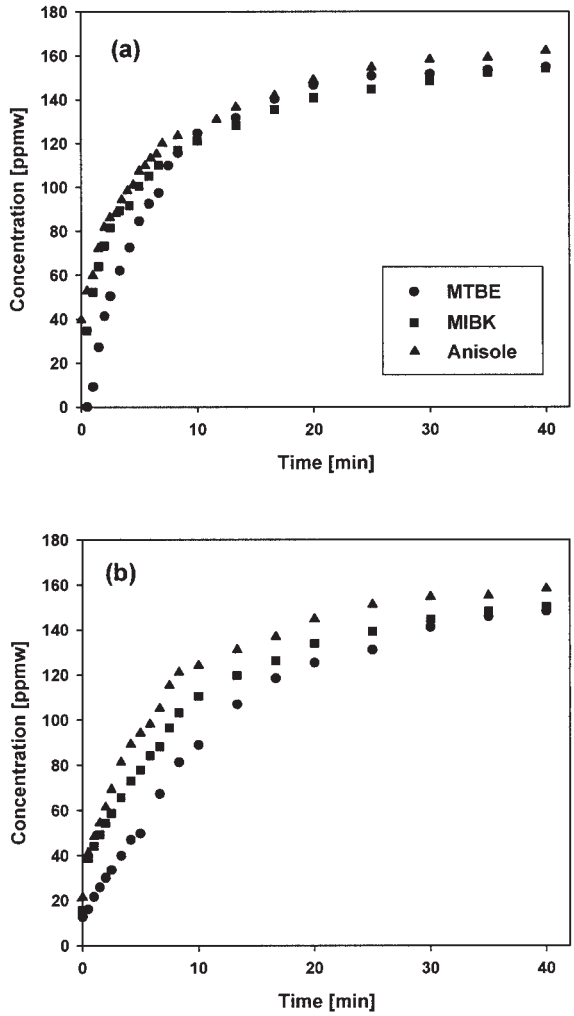

Figure 13. Re-Adsorption breakthrough curves by using sample 11 (flow rate = 1.0 ml/min); effect of desorbent (a) at 303 K and (b) at 323 K.

Acknowledgments

This work is supported by the Ministry of Environment as "The Ecotechnopia 21 project" and SK Co. The authors would like to thank the Ministry of Environment and SK Co.

Notation

$C_{\mu s}$ = concentration of the liquid phase (mol/cm^3)
C_{μ} = concentration of the adsorbed phase (mol/cm^3)
$C_{\mu s}$ = maximum adsorbed concentration (mol/cm^3)
D_e = effective diffusivity (cm^2/s)
F = fractional uptake (−)
R_p = radius of a pellet (cm)
t = time (s)

Superscripts and Subscripts

μ = adsorbed phase

Literature Cited

1. Min W. A unique way to make ultra low sulfur diesel. *Korean J Chem Eng.* 2002;19:601-606.
2. Hernández-Maldonade AJ, Yang RT. Desulfurization of diesel fuels by adsorption via π-complexation with vapor-phase exchanged Cu(I)-Y zeolites. *J Am Chem Soc.* 2004;126:992-993.
3. Gates BC, Topsøe H. Reactivities in deep catalytic hydrodesulfurization: challenges, opportunities, and the importance of 4-methyldibenzothiophene and 4,6-dimethyldibenzothiophene. *Polyhedron.* 1997;16:3213-3217.
4. Ho TC. Inhibiting effects in hydrodesulfurization of 4,6-diethyldibenzothiophene. *Journal of Catalysis.* 2003;219:442-451.
5. Wiwel P, Knudsen K, Zeuthen P, Whitehurst DD. Assessing compositional changes of nitrogen compounds during hydrotreating of typical diesel range gas oils using a novel preconcentration technique coupled with gas chromatography and atomic emission detection. *Ind Eng Chem Res.* 2000;39:533-540.
6. Zeuthen P, Knudsen KG, Whitehurst DD. Organic nitrogen com-

pounds in gas oil blends, their hydrotreated products and the importance to hydrotreatment. *Catal Today.* 2001;65:307-314.
7. Murti SDS, Yang H, Choi KH, Korai Y, Mochida I. Influences of nitrogen species on the hydrodesulfurization reactivity of a gas oil over sulfide catalysts of variable activity. *Appl Catal A: General.* 2003;252: 331-346.
8. Yang RT, Hernández-Maldonade AJ, Yang FH. Desulfurization of transportation fuels with zeolites under ambient conditions. *Science.* 2003;301:79-81.
9. Yang RT. *Adsorbents: Fundamentals and Applications*. New York: Wiley; 2003.
10. Hernández-Maldonade AJ, Yang RT. Denitrogenation of transportation fuels by zeolites at ambient temperature and pressure. *Angew Chem Int Ed*. 2004;43:1004-1006.
11. Kim S, Kim YK. Apparent desorption kinetics of phenol in organic solvents from spent activated carbon saturated with phenol. *Chemical Engineering Journal.* 2004;98:237-243.
12. Dąbek L. Sorption of zinc ions from aqueous solutions on regenerated activated carbons. *J Hazardous Materials*. 2003;B101:191-201.
13. Reid RC, Prausnitz JM, Poling BE. *The Properties of Gases and Liquids*. Singapore: McGraw-Hill, Inc.; 1988.
14. Suzuki M. *Adsorption Engineering*. Tokyo: Elsevier; 1990.
15. Morterra C, Orio L, Emanuel C. Infrared spectroscopic surface characterization of zirconium oxide, Part 3. The CO/CO_2 and CO/H_2O interactions at the surface of a high-area monoclinic preparation. *J Chem Soc Faraday Trans.* 1990;86:3003-3013.
16. Infantes-Molina A, Mérida-Robles J, Maireles-Torres P, Finocchio E, Busca G, Rodríguez-Castellón E, Fierro JLG, Jiménez-López A. A new low-cost synthetic route to obtain zirconium containing mesoporous silica. *Microporous and Mesoporous Materials.* 2004;75:23-32.
17. Ng KC, Chua HT, Chung CY, Loke CH, Kashiwagi T, Akisawa A, Saha BB. Experimental investigation of the silica gel-water adsorption isotherm characteristics. *Applied Thermal Engineering.* 2001;21:1631-1642.

Manuscript received Mar. 22, 2005, and revision received Jun. 21, 2005.